dicarbazolylpropane and Professor E. P. Kyba and his group at The University of Texas at Austin for their help in synthesizing the 1,3-dinaphthylpropane.

References and Notes

(1) Ishii, T.; Handa, T.; Matsunaga, S. *J. Polym. Sci., Polym. Phys. Ed.* **1979**, *17*, 811.

(2) Pfister, G.; Williams, D. J.; Johnson, G. E. *J. Phys. Chem.* **1974**, *78*, 2009.

(3) (a) Hoyle, C. E.; Nemzek, T. L.; Mar, A.; Guillet, J. E. *Macromolecules* **1978**, *11*, 429. (b) Ghiggino, K. P.; Wright, R. D.; Phillips, D. *Chem. Phys. Lett.* **1978**, *53*, 552 [poly(1-vinylnaphthalene)]. *Eur. Polym. J.* **1978**, *14*, 567 (PVCz).

(4) Johnson, G. E. *J. Chem. Phys.* **1975**, *62*, 4697.

(5) Johnson, G. E. *J. Chem. Phys.* **1975**, *63*, 4047.

(6) Roberts et al. (Roberts, A. J.; Cureton, C. G.; Phillips, D. *Chem. Phys. Lett.* **1980**, *55*, 554) have argued that the decay at 360 nm required a three-exponential fit. Our signal-to-noise ratio would not allow a meaningful fit of this type to be undertaken.

(7) This follows the kinetic scheme of Johnson as applied to PVCz.[4] More recent work[6,23] has suggested that the fluorescence decay in the monomer region is more complex than a simple monomer–excimer dissociation. Our experimental precision is not adequate to detect these small differences and the biexponential form is able to provide a reasonably good fit to the experimental data.

(8) Chandross, E. A.; Dempster, C. J. *J. Am. Chem. Soc.* **1970**, *92*, 3586.

(9) Frank and Hurrah (Frank, C. W.; Hurrah, L. A. *J. Chem. Phys.* **1974**, *61*, 1526) have estimated that the fraction of preformed excimer pairs in P2VN at 20 °C is approximately 10^{-2}. (b) Similarly Klöpffer (Klöpffer, W. *J. Chem. Phys.* **1969**, *50*, 2337) has estimated this fraction to be 10^{-3} for PVCz, based on his fluorescence quenching data.

(10) Irie, M.; Kamijo, T.; Aikawa, M.; Takemura, T.; Hayashi, K.; Baba, H. *J. Phys. Chem.* **1977**, *81*, 1571.

(11) These results have been presented eariler in ref 1 and 2. Reference 1 has the full quenching expressions for the case in which k_d cannot be ignored.

(12) The data plotted in Figures 4 and 5 is an average of several wavelengths in the monomer and excimer region (e.g., for P2VN, use 330–350 nm for M and 400–460 nm for D). The Stern–Volmer constants for this averaged data are essentially the same as the average of the Stern–Volmer constants for the data at each wavelength treated independently.

(13) All least-squares fits were done by using the MINITAB statistical package installed on The University of Texas computer system.

(14) This is in contradiction to ref 2, where relations 6 and 7 were used to obtain K_{SV}^{M} and K_{SV}^{D} for PVCz quenching by trichloro- and tribromoacetic acid. In ref 2 quencher concentrations up to 10× the present work were used. An analysis like ref 2 was used in ref 15 for quenching by dimethyl terephthalate.

(15) Itaya, A.; Okamoto, K.; Kusabayashi, S. *Bull. Chem. Soc. Jpn.* **1976**, *49*, 2082.

(16) (a) Birks, J. B. "Photophysics of Aromatic Molecules"; Wiley-Interscience: New York, 1970. (b) Birks, J. B.; Dyson, D. J.; Munro, I. H. *Proc. R. Soc. London, Ser. A* **1963**, *275*, 575.

(17) Tagawa, S.; Washio, M.; Tabata, Y. *Chem. Phys. Lett.* **1979**, *68*, 276. A 10-ps-wide, 35-MeV electron beam was used as an excitation source in this reference.

(18) Voltz, R.; Laustriat, G.; Coche, A. *J. Chim. Phys. Phys.-Chim. Biol.* **1966**, *63*, 1253.

(19) Assumptions of this type have been made by a number of authors. See ref 1 for example. Also see: (a) Abuin, E. A.; Lissi, E. A.; Gargallo, L.; Radic, D. *Eur. Polym. J.* **1979**, *15*, 373. (b) Ishii, T.; Handa, T.; Matsunaga, S. *Macromolecules* **1978**, *11*, 40.

(20) Because of the larger physical size of DCP, it is reasonable to assume that $D_{DCP} < D_{EtCz}$. However, singlet energy transfer can occur between the two chromophores, such that $R_{DCP} > R_{EtCz}$. Thus if $P_{DCP} \approx P_{EtCz}$, the net quenching rates would be expected to be comparable. A similar argument can be made for DNP.

(21) Holden, D. A.; Guillet, J. E. *Macromolecules* **1980**, *13*, 289.

(22) Klöpffer[9b] estimated Λ_s to be on the order of 200 Å for films of PVCz. Presumably this larger Λ_s value reflects the absence of chromophore mobility in solution, which can produce a singlet exciton trap during the lifetime of PVCz-M.

(23) Holden, D. A.; Wang, P. Y.-K.; Guillet, J. E. *Macromolecules* **1980**, *13*, 295.

Kinetics of Doping and Degradation of Polyacetylene by Oxygen

J. M. Pochan,* D. F. Pochan, H. Rommelmann, and H. W. Gibson

Webster Research Center, Xerox Corporation, Webster, New York 14580.

Received June 19, 1980

ABSTRACT: The kinetics of oxidative degradation of various cis/trans compositions of polyacetylene have been studied. It has been shown that the degradation process follows an initial doping that is normally observed for polyacetylene with other electron acceptors. The kinetics of degradation are first order and have been modeled with consecutive reaction theory. Two first-order rate constants are observed with higher trans content materials (>50% trans). For a given trans content, the rate constants provide identical activation energies. The activation energies range from ~9 (30 and 60% trans) to 13.8 kcal/mol (~98% trans). Simultaneous conductivity–oxygen uptake experiments indicate maximum conductivity at 0.14 O_2 molecules per -CH=CH- unit. These results indicate the absolute necessity for an oxygen-free environment to obtain the intrinsic electrical properties of this interesting polymer.

The doping of polyacetylene [(-CH=CH-)$_n$] to highly conductive metallike behavior has recently been the subject of intense study.[1-5] Such dopants as the halogen gases,[5] AsF_5, BF_3, BCl_3, SO_2, NO, and HCN[1] have been studied. With the exception of one paper,[1] the effect of oxygen, which is a pervasive electron acceptor, has not been studied. In that paper, (-CH=CH-)$_n$ was prepared with an oxygen content as low as 0.7 wt %. It was noted that exposure to oxygen for long time periods caused irreversible chemical changes in the material. Unfortunately, those studies were conducted on compressed powder pellets of (-CH=CH-)$_n$ and results are difficult to extrapolate to continuous films. Since the oxidative degradation process can have profound effects on the ultimate properties of (-CH=CH-)$_n$, we have undertaken a study on the effect of oxygen on the conductivity and the kinetics of degradation of continuous polyacetylene films. Preliminary accounts of this work have appeared.[6-8]

Experimental Section

Polyacetylene was prepared by the method of Shirakawa[9] and was approximately 160-μm thick. Samples were stored in an O_2-free environment (<0.8 ppm). Initially, the sample was 90% cis as determined by infrared measurements. Various cis/trans ratios were obtained via thermal treatment. A 98% trans sample was made by heating a cis sample at 200 °C for 3 h in an argon atmosphere. Cis–trans ratios cited are prior to oxidation.

0024-9297/81/2214-0110$01.00/0

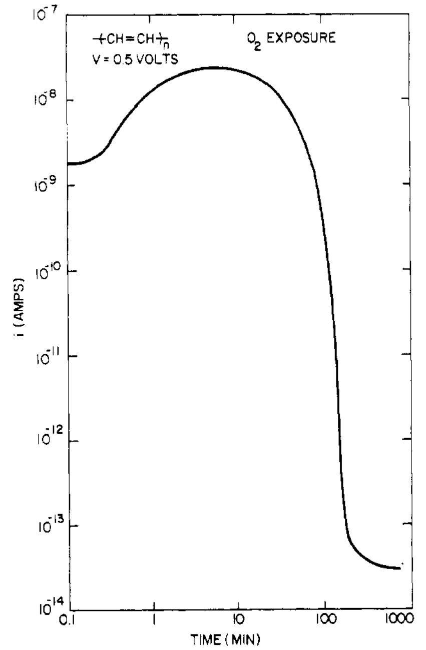

Figure 1. log-log plot of current vs. exposure time to pure O_2 for a sample of 60% *trans*-polyacetylene. $T = 342.6$ K.

Electrical measurements were made on the free-standing films two ways: (1) The film was transferred from an oxygen-free environment to a Balzar evaporation system, where $\sim 10^3$-Å gold electrodes were evaporated onto its surface. It was then transferred to a stainless steel flow cell in which various gases could be circulated. The cell was spring loaded in a two-electrode configuration. This experiment permitted exposures of the samples to ~1 min of air. (2) In the other method, the film was transferred directly to the flow cell in an oxygen-free argon environment and contact made in the two-electrode configuration. Ohmic contacts were observed with solder-stainless steel contacts as well as with the gold-evaporated electrodes prior to and after exposure to oxygen. Conductivity experiments were performed by monitoring current with a Keithley 616 electrometer in series with the sample and a Keithley high-voltage regulated power supply. Guard rings were not used in the experimental configuration as they have been shown to have little effect on results.[1] The sample cell was temperature regulated with a Delta Design Environmental Oven. The gas feed to the cell was circulated in the oven prior to cell entrance to ensure thermal equilibration.

Degradation experiments were conducted by thermally equilibrating the sample in flowing argon and then introducing oxygen and monitoring current as a function of time.

Additional experiments to monitor current and oxygen uptake simultaneously were performed by replacing the flow cell with a glass vacuum system with electrical feedthroughs. Electrical contacts were identical with those in the flow cell. The system, including the sample, was degassed and volume calibrated by using known volumes of argon and the ideal gas law. Pressure in the system was measured with an MKS Instruments, Inc., Baratron with a 0-1000-torr pressure head. A known pressure of oxygen was introduced to the system and current and pressure were monitored as a function of time. As the oxyygen was sorbed into the sample, a pressure drop resulted. This pressure drop along with the calibrated volume was used to calculate the moles of oxygen sorbed (via the ideal gas law). Typically, the pressure drop was less than 0.5% of the initial pressure; thus, the oxygen concentration was essentially constant.

Results and Discussion

A. Kinetic Treatment. The effect of oxygen exposure on the conductivity of polyacetylene is shown in Figure 1, where it is seen that initial exposure increases the conductivity and then decreases it dramatically with time. The curve is characteristic of all polyacetylene samples exposed to oxygen at various temperatures. The data are not unlike those for bromine doping, but the effect is much more dramatic.[3]

The data in Figure 1 are reminiscent of those observed in many consecutive chemical reaction schemes:

$$\mathrm{A} \xrightarrow{k_1} \mathrm{B} \xrightarrow{k_2} \mathrm{C} \qquad (1)$$

In eq 1 A, B, and C represent the relative numbers of each chemical species and k_1 and k_2 are rate constants for each individual reaction; i.e., A going to B and B going to C. The analogy to eq 1 as regards polyacetylene in oxygen would be written

$$(\text{-CH=CH-})_n + \mathrm{O_2} \underset{k_3}{\overset{k_1}{\rightleftharpoons}} (\text{CH=CH}/\mathrm{O_2})^+ \xrightarrow{k_2} \text{products} \qquad (2)$$

where k_1 is the rate of formation of a polyacetylene-oxygen complex that produces increased conductivity and k_2 is the rate constant for degradation of this complex to a nonconductive product. k_3 must be included in this reaction scheme as it has been shown that during certain experimental circumstances the oxygen doping of polyacetylene is reversible.[1,6,8] In our case, k_3 is extremely small.[6] If $k_1 \gg k_2$ and k_3 in eq 2 and the diffusion of oxygen into the polyacetylene film is rapid, the degradation of the conductive complex becomes rate limiting in a current (conductivity) measurement. Then

$$\mathrm{d[complex]}/\mathrm{d}t \propto \mathrm{[complex]} = k_2\mathrm{[complex]} \qquad (3)$$

where the bracketed quantity is the number of complex molecules. Equation 3 is a first-order rate equation[10] whose solution is exponential; i.e.

$$\mathrm{[complex]} = \mathrm{[complex]}_0 e^{-t/\tau} \qquad (4)$$

where t is time and τ is the time constant for the reaction.

B. Conducting Model. Equation 2 can be coupled with a simple parallel resistance model to explain the observed results. Assume at any time t during the oxygen exposure cycle that the system is composed of three resistive species: the uncomplexed polymer (R_u), the complexed polymer (R_c), and the oxidation product (R_p). The resistance of the total system can be written

$$\frac{1}{R_t} = \frac{N_u}{R_u} + \frac{N_c}{R_c} + \frac{N_p}{R_p} \qquad (5)$$

where N_u, N_c, and N_p represent the fraction of each of the species present. Admittedly, this model is simple considering the complexity of the polymer's fibril morphology and ordered character, but, as will be seen, the model provides a qualitative description of the results. In these experiments, $R_p >>> R_c$ and R_u. The oxidized samples exhibit conductivities 4-6 orders of magnitude lower than those of the intrinsic polymer or the complexed state. R_u is at least 1 order of magnitude greater than R_c.[6] It is difficult to tell the exact ratio of R_u and R_c as degradation of the polymer begins before steady-state conductivity is achieved. We have observed increases of 2-3 orders of magnitude in polyacetylene conductivity with initial oxygen doping and assume for these calculations that R_c is at least 3 orders of magnitude less than R_u. If eq 5 is considered with these assumptions, the term N_c/R_c controls the conductivity when the maximum in the current-exposure time occurs. Since current is being measured in these experiments, eq 5 can be rewritten

$$i = V/R_t \approx VN_c/R_c \qquad (6)$$

where V is the voltage applied and i the current measured.

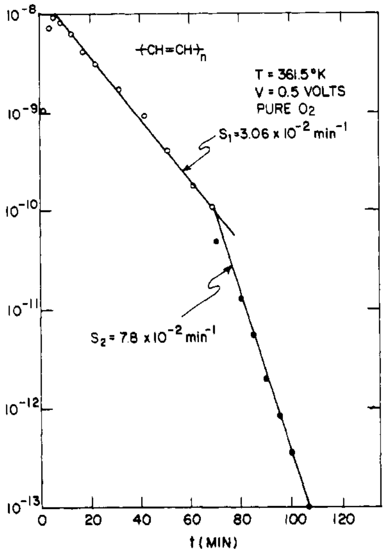

Figure 2. log (current) vs. exposure time to pure O_2 for a sample of 60% *trans*-polyacetylene. T = 361.5 K.

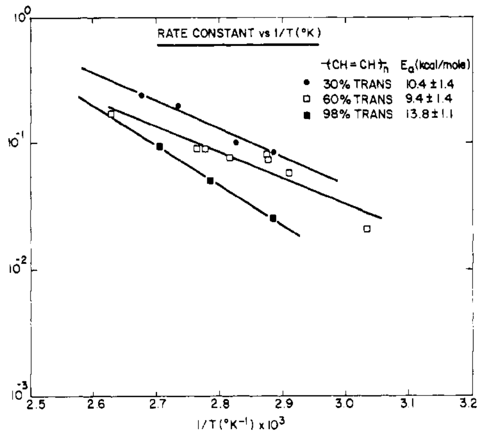

Figure 3. log (rate constant) (S_2) (min^{-1}) vs. inverse temperature for 30, 60, and >98% *trans*-polyacetylene.

We have discussed earlier the first-order decay of the complexed species and we can write eq 6 as

$$i = \frac{V}{R_c} N_{c_0} e^{-t/\tau} \qquad (7)$$

The current decay should exhibit first-order decay behavior if the above assumptions are correct.

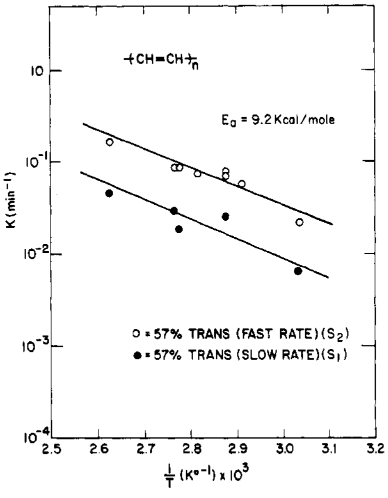

Figure 4. log (rate constant) (S_1 and S_2) (min^{-1}) vs. inverse temperature for a 57% *trans*-polyacetylene.

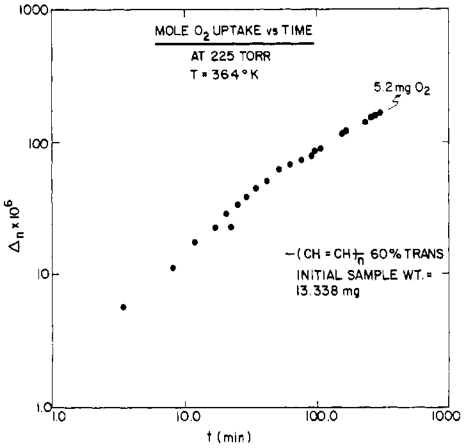

Figure 5. Moles of oxygen sorbed vs. time for a 13.338-mg sample of 60% *trans*-polyacetylene. T = 364 K, $P \sim 225$ torr of pure O_2.

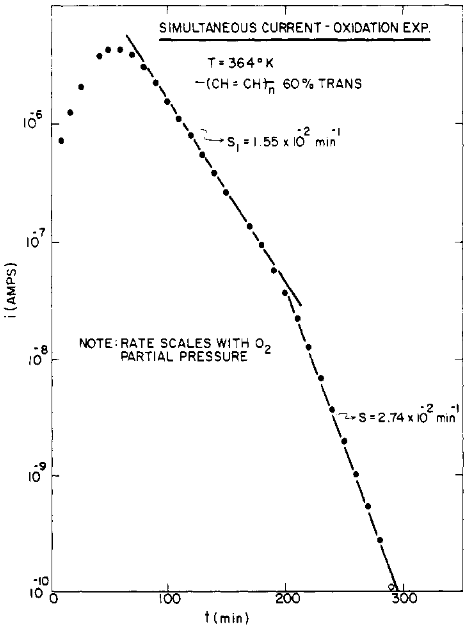

Figure 6. log (current) vs. time for a 60% *trans*-polyacetylene sample exposed to $\sim$ 225 torr of pure O_2 at 364 K. V = 100 V.

Figure 2 is a semilog plot of data similar to Figure 1 and it is seen that the data are linear with two slopes (S_1 and S_2). The conductivity values are within a half order of magnitude of the current levels shown in the figure. This two-process behavior has been observed in 60 and ~98% trans samples but it is not observed in a 30% trans sample, where only a single rate constant is observed during the entire experiment. (This observation will be discussed later when a chemical resistivity model is proposed for this degradation.) If τ in eq 4 is thermally activated, i.e., $\tau = \tau_0 e^{E_a/kT}$, a plot of S_1 or S_2 vs. inverse temperature should provide an activation energy. A plot of S_2 vs. $1/T$ is shown in Figure 3 for the various samples. The rate data for the 70% cis sample are included in this plot. It is seen that degradation is Arrhenius activated. The activation energy and rate constants are functions of the cis/trans ratio. The higher the cis content in the system, the higher the rate constant. S_1 and S_2 are plotted vs. inverse temperature in Figure 4 for the 60% trans sample. Within the limits of error, an identical activation energy is obtained for S_1 and S_2.

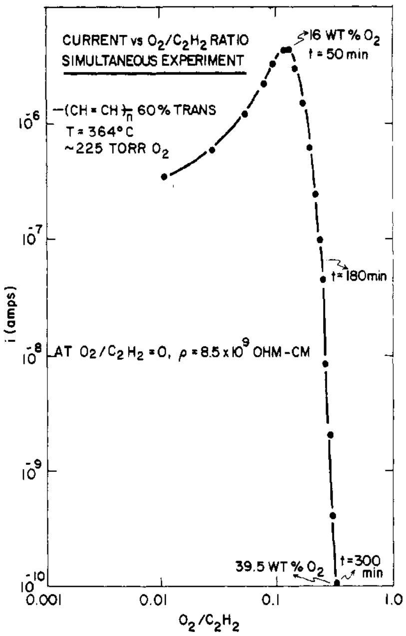

Figure 7. log–log plot of current vs. O_2/C_2H_2 molar ratio during simultaneous current–sorption experiment. Sample is 60% trans. $V = 100$ V.

Figures 5 and 6 show data taken simultaneously during a degradation experiment. In Figure 5, the initial time dependence for the oxygen sorption is linear (t^1) and not characterized by a normal $t^{1/2}$ diffusion, but by diffusion followed by a chemical reaction (complexation).[11,12] The change in slope at ~60 min to a $\sim t^{1/2}$ dependence corresponds to the maximum in the current vs. time curve. As oxidation proceeds it would be expected that the sorption process would approach an asymptotic limiting value. The corresponding current vs. time curve exhibits the double rate process behavior. It is interesting to note that no discontinuity in the uptake curve (Figure 5) exists in the region where the current decay curve changes slope. Thus, the oxygen sorption process is not changing detectably, but the process of conduction is. This point will be addressed shortly.

The data from Figures 5 and 6 are plotted together in Figure 7 as current vs. the O_2/C_2H_2 molar ratio. The peak in the curve corresponds to 0.14 oxygen molecules per double bond of the polymer. The weight percent values are also shown in the figure. The results indicate that an oxygen level of approximately one atom per 10 double bonds is sufficient to begin disrupting the conductivity of these samples.

When dry air or a partial atmosphere of oxygen was used in these experiments, the measured rate constants scaled with the oxygen partial pressure. Such a result is consistent with the proposed kinetic schemes of eq 2 and 3 since [complex] = $k_1[\text{-(CH=CH-)}_n][O_2]$; i.e., the reaction is first order in oxygen.

Equation 7 does not explain the two apparent rate processes observed in the high *trans*-polyacetylene cases. There are two possible explanations. The first is that the conductive species has not reached maximum concentration prior to the point at which the degradative process is appreciable. This is shown schematically in Figure 8, where the concentration of the various species is shown as a function of time. In Figure 8A, N_c has reached its maximum prior to the formation of any oxidative products. If our assumptions are correct, eq 7 would then be expected to describe the decay process. In Figure 8B, major degradation begins to occur prior to N_c reaching maximum; i.e., $k_1 \sim k_2$ in eq 1. If this case occurs (as might be the case in a diffusion-limited process), then the concentration of conductive species is still increasing while oxidation takes place. In this time region, where both doping and degradation are occurring simultaneously, the decay curve would have a lower slope then would be observed if a maximum in the complex concentration had already been attained (S_1 in Figure 2). In such a situation, the linearity of S_1 in plots such as Figure 2 would only be apparent in view of the S-shaped curves generated with the constraint $k_1 \sim k_2$.[13]

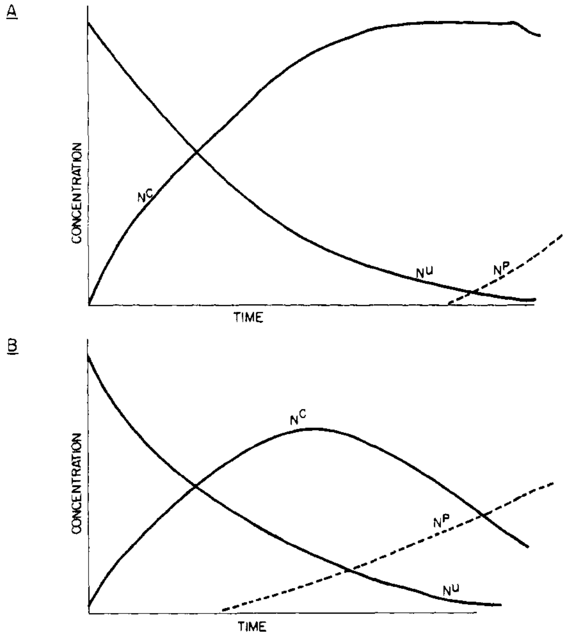

Figure 8. Schematic of the concentration profiles of N_u, N_c, and N_p as a function of time: (A) $k_1 >>> k_2$ in eq 2; (B) $k_1 \sim k_2$ in eq 2.

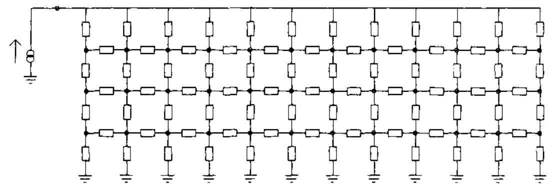

Figure 9. Cross-linked circuit model used for theoretical degradation model.

The second possibility could be associated with the morphology and cross-linked structure of the polyacetylene. Instead of the network being considered completely parallel, a network such as shown in Figure 9 could occur. The resistances represent a simplification of either molecular cross-links or fibril crossovers that could control the observed conductivity. For simplicity, all R's are considered identical. The degradative decay of the system shown in Figure 9 was theoretically modeled in the following manner. Each resistor in the circuit was assigned a number and given a resistance of 1 Ω. A computer random number generator was used to choose which of the resistances degraded to an arbitrary value of 10^4 Ω. Any resistor that had previously "reacted" was ignored. Log (effective current) ($1/R$) was then plotted as a function of time (reaction events). The average results of four experiments are shown in Figure 10, where it is seen that, as resistors are eliminated from the circuit, the effective conductivity drops slowly until a critical reaction point is attained, where a precipitous drop occurs. If the resistance of the reacted sites were larger, the change occurring near

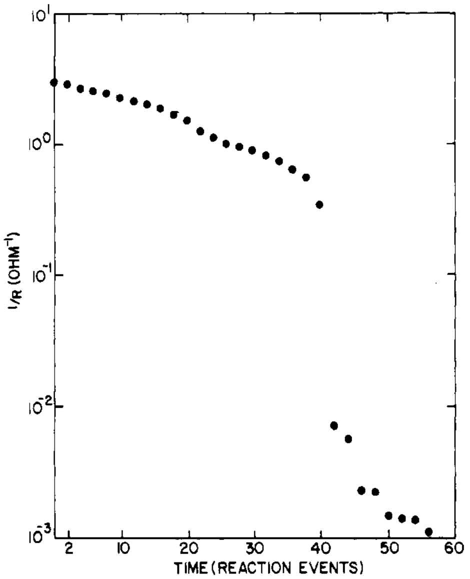

Figure 10. log (effective current) ($1/R$) vs. time for theoretical degradation model.

a time of "40" would be larger. (Naturally, a larger network in the model would "smooth" the data in Figure 10, especially the region where conducitivity is dropping precipitously.) The result qualitatively describes the kinetics observed during our experiments.

A question arises as to whether we are describing a morphological effect (interfibril contact) or an intermolecular (interchain) effect. Interchain overlaps would be expected to provide a more intimate contact between conductors than the morphological overlap of $(\text{-CH=CH-})_n$ fibrils. On the basis of this we feel that if the morphological rather than the kinetic model is correct, the two-rate process observed during the oxidative degradation is caused by interfibril contacts.

C. Relation of Cis-Trans Ratio and Oxidation. Degradation rates for polyacetylene are slow at ambient conditions and all experiments were thus carried out at elevated temperatures where the cis → trans conversion leads to generation of a relatively stable free-radical population which is probably caused by the breaking of cis double bonds as they rearrange to trans. During this conversion, free-radical oxidation of the polymer can occur. With these conditions, the higher percentage cis samples would oxidize at a higher rate and this is what is observed. Most probably this reaction is taking place during doping and cannot be observed due to the overlapping doping and degradation processes. A well-annealed, almost totally converted trans sample would still be expected to undergo similar reactions as all the converted cis double bonds could not be expected to recombine in the trans state. The so-called soliton phase kink may not be removed via thermal treatment.[13] We thus feel that the oxidation of polyacetylene is intimately related to the cis → trans isomerization and phase inversion positions of the polymer which can readily oxidize. The possibility of a singlet oxygen interaction with the polyene structure cannot be eliminated, but we do note that all experiments were conducted in the dark and that transported oxygen was flowing through an ultraviolet absorber (Tygon) so that production of singlet oxygen was minimized.[15]

Conclusion

The kinetics of oxidative degradation of various cis-trans compositions of polyacetylene have been studied. It has been shown that the degradation process follows an initial doping that is normally observed for polyacetylene with other electron acceptors. The kinetics of degradation are first order and have been modeled with consecutive reaction theory. Two first-order rate constants are observed with higher trans content materials (>50% trans). A morphological and/or chemical kinetic model can be used to explain these rate constants. For a given trans content, the two rate constants provide identical activation energies. The activation energies range from ~9 (30 and 60% trans) to 13.8 kcal/mol (~98% trans). Simultaneous conductivity-oxygen uptake experiments indicate maximum conductivity at 0.14 O_2 molecules per -CH=CH- unit. These results indicate the absolute necessity for an oxygen-free environment to obtain the intrinsic electrical properties of this interesting polymer.

References and Notes

(1) Berets, D. J.; Smith, D. S. *Trans Faraday Soc.* **1968**, *64*, 823.
(2) Shirakawa, H.; Ito, T.; Ikeda, S. *Makromol. Chem.* **1978**, *179*, 1565.
(3) Chiang, C. K.; Park, Y. W.; Heeger, A. J.; Shirakawa, H.; Louis, E. J.; MacDiarmid, A. G. *J. Chem. Phys.* **1978**, *69*, 5098.
(4) Chiang, C. K.; Gau, L. C.; Fincher, G. R., Jr.; Park, Y. W.; MacDiarmid, A. G.; Heeger, A. J. *Appl. Phys. Lett.* **1978**, *33*, 18.
(5) Shirakawa, H.; Louis, E. J.; MacDiarmid, A. G.; Chiang, C. K.; Heeger, A. J. *J. Chem. Soc., Chem. Commun.* **1977**, 578.
(6) Pochan, J. M.; Bailey, F. C.; Gibson, H. W. *J. Polym. Sci., Polym. Lett. Ed.* **1980**, *18*, 447.
(7) Pochan, J. M.; Gibson, H. W.; Bailey, F. C.; Pochan, D. F. *Polymer* **1980**, *21*, 250.
(8) Pochan, J. M.; Gibson, H. W. *Org. Coat. Plast. Chem.* **1980**, *42*, 600.
(9) Ito, T.; Shirakawa, H.; Ikeda, S. *J. Polym. Sci., Polym. Chem. Ed.* **1974**, *12*, 11.
(10) Moore, Walter J. "Physical Chemistry"; Prentice-Hall: Englewood Cliffs, N.J., 1962; p 267.
(11) Danckwerts, P. V. *Trans. Faraday Soc.* **1950**, *46*, 300.
(12) Nysing, R. A. T. O. Absorptie van gassen Vloeistoffen, Zonder en met Chemische Reactie, Academisch Proefschrift, Delft, 1957.
(13) Frost, A.; Pearson, R. G. "Kinetics and Mechanism", 2nd ed.; Wiley: New York, 1962; p 166.
(14) Goldberg, I. B.; Crowe, H. R.; Newman, P. R.; Heeger, A. J.; MacDiarmid, A. G. *J. Chem. Phys.* **1979**, *70*, 1132.
(15) Rånby, R.; Rabek, J. F. "Singlet Oxygen—Reactions with Organic Compounds and Polymers"; Wiley: New York, 1978; Chapter 21.